



Journal of Environmental Science and Technology

ISSN 1994-7887

science
alert

ANSI*net*
an open access publisher
<http://ansinet.com>

Synthetic Textile Effluent Removal by Skin Almonds Waste

F. Atmani, A. Bensmaili and N.Y. Mezenner
Laboratoire de Génie de la Réaction,
Faculté de Génie Mécanique et Génie des Procédés,
Université des Sciences et de la Technologie Houari Boumediene,
BP 32 El-Alia Bab Ezzouar, Alger, Algeria

Abstract: In the present study, natural and treated skin almonds were used as adsorbents for adsorption kinetics of methyl orange (acid dye) and crystal violet (basic dye). Skin almonds were treated by three different types of chemical treatments: acidic treatment (H_2SO_4), alkaline treatment (NaOH) and salt treatment ($MgCl_2$). The maximum adsorption capacities of crystal violet onto skin almond and methyl orange onto natural and treated skin almond with H_2SO_4 were 85.47, 15 and 31.94 $mg\ g^{-1}$, respectively, at 23°C. Untreated skin almonds might be a good adsorbent for the removal of basic dye from water solution. The fitness of both Langmuir and Freundlich adsorption model on describing the equilibrium isotherms of Crystal Violet (CV) and Methyl Orange (MO) were examined. The experimental data fitted very well the pseudo second order kinetic model and also followed by intraparticle diffusion model. The results show that the sorption capacity decreases with an increase in solution temperature from 23 to 50°C. The thermodynamics parameters were evaluated. The negative value of enthalpy (ΔH°) indicated that the adsorption of both dye onto skin almonds were exothermic, which result was supported by the decreasing adsorption of dye with temperature.

Key words: Dye, low-cost adsorbent, adsorption, kinetic study, thermodynamic

INTRODUCTION

Dyes are extensively used in paper, textile, dye-houses and printing to color the final products (Aksu, 2005). They usually have a synthetic origin and complex aromatic structures making them difficult to degraded (Aksu and Tezer, 2005). Dyes are classified as anionic, cationic and nonionic dyes (Fu and Viraraghavan, 2001). Existing colored wastewater treatment methods involve in a combination of physical and chemical processes. Adsorption is one of the effective methods to remove colored textile contaminants from wastewater. Recently, attentions have been focused on the development of low cost adsorbent for the application concerning treatment of wastewater (Namasivayam *et al.*, 2001; Forgacs *et al.*, 2004; Gurses *et al.*, 2006; Hamdaoui, 2006; Grini *et al.*, 2007). In the last 3 years, our laboratory has developed fast and cost effective methods for the removal of metals using waste materials like egg shells (Yeddou and Bensmaili, 2007). Skin almonds, being a low-cost and easily available adsorbent, could be an alternative for more costly wastewater treatment

Corresponding Author: Fatiha Atmani, Laboratoire de Génie de la Réaction,
Faculté de Génie Mécanique et Génie des Procédés,
Université des Sciences et de la Technologie Houari Boumediene,
BP 32 El-Alia Bab Ezzouar, Alger, Algeria Tel/Fax: 21321247919

processes. To the best of our knowledge, there is no information in literature on the use of skin almonds as an adsorbent. In this study, the potentials for the use of skin almonds as an adsorbent for crystal violet and methyl orange removal from solution were investigated.

The objective of this study was to explore the feasibility of using Skin Almonds (SA), a new agriculture sorbent for removal of crystal violet and methyl orange.

MATERIALS AND METHODS

The study was conducted at the Laboratory of chemical reaction, Faculty of Mechanical Engineering and Process of Engineering, Houari Boumediene University of Science and Technology, Algiers, Algeria (USTHB) During 2008.

Adsorbate

The basic dye crystal violet and the acid dye methyl orange are widely used in the textile, pharmaceutical and paper manufacturing. Double distilled water was employed for preparing all the solutions.

Adsorbent

Before use, the skin almonds were washed in distilled water for several times and dried at 100°C for 2 h. After drying, the skin almond was sieved to obtain a particle size range of 0.1-0.25 mesh. Studies were carried out using two different forms of skin almonds, natural (designated as NSA) and treated (designated as TSA). In order to enhance the adsorption aptitudes of these adsorbent, different types of chemical treatments: acidic treatment (H₂SO₄), alkaline treatment (NaOH) and salt treatment (MgCl₂) were investigated. Activation will increase the surface area and the fraction of mesopore volume simultaneously (Wua *et al.*, 2005). One hundred grams of skin almonds was mixed with solution of reagent. The mixture was stirred for different times (Table 1) after which it was washed several times with distilled

Table 1: Operating conditions of the treatment of skin almonds

Solution of reagent	Temperature (°C)	Concentration (mol L ⁻¹)	Treatment time (h)
H ₂ SO ₄ 1	70	2	4
H ₂ SO ₄ 2	70	2	2
H ₂ SO ₄ 3	50	2	4
H ₂ SO ₄ 4	50	2	2
H ₂ SO ₄ 5	70	1	4
H ₂ SO ₄ 6	70	1	2
H ₂ SO ₄ 7	50	1	4
H ₂ SO ₄ 8	50	1	2
NaOH 1	70		4
NaOH 2	70	2	2
NaOH 3	50	2	4
NaOH 4	50	2	2
NaOH 5	70	2	4
NaOH 6	70	1	2
NaOH 7	50	1	4
NaOH 8	50	1	2
MgCl ₂ 1	70	2	4
MgCl ₂ 2	70	2	2
MgCl ₂ 3	50	2	4
MgCl ₂ 4	50	2	2
MgCl ₂ 5	70	1	4
MgCl ₂ 6	70	1	2
MgCl ₂ 7	50	1	4
MgCl ₂ 8	50	1	2

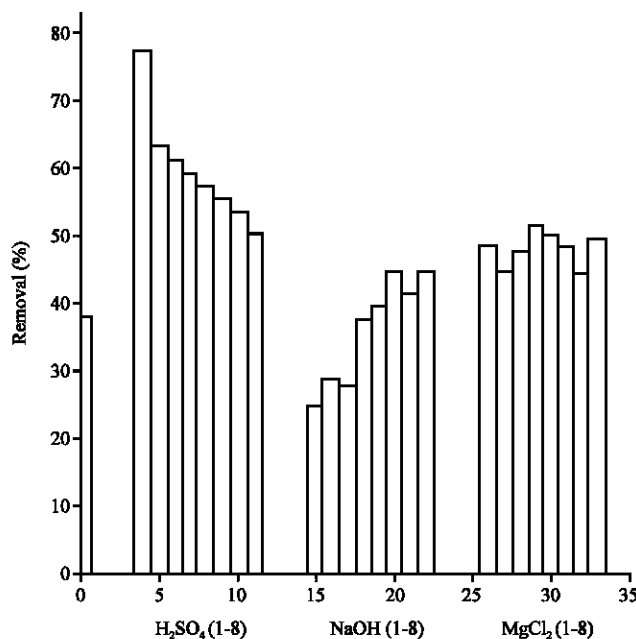


Fig. 1: Effect of chemical treatment on the adsorption of methyl orange

water and filtrated; the optimization of chemical treatment operating conditions such as: temperature, contact time and chemical concentration of solution reagent were investigated.

Figure 1 and 2 show the results for the removal of crystal violet and methyl orange by natural and treated skin almonds. Among the different chemical treatment used, treatment with H₂SO₄ is the most effective for skin almonds. It was observed from Fig. 1, that the percentage of removal of methyl orange increases from 37.5-78.12% for the treatment by H₂SO₄ (Temp. is 70°C and treatment time of 4 h). Little increase of the adsorption capacity of the tested skin almonds was obtained by NaOH (37.5 to 45%) and MgCl₂ (37.5 to 52%). Figure 2 shows that the effect of treatment of skin almonds on the removal of crystal violet was not significant. Consequently, methyl orange removal studies were carried out using different skin almonds forms, natural and treated.

Equilibrium Studies

Sorption Isotherms

Adsorption experiments were carried out by adding a fixed amount of adsorbent (0.3 g) to a series of conical flasks filled with 50 mL diluted dye solutions. The conical flasks were placed in a thermostatic shaker for crystal violet and methyl orange, respectively. The adsorption amount on natural and modified skin almonds was calculated indirectly from the difference of dye concentration in solution before and after the experiment. The dye concentration was determined by measuring the absorbance of the solution using U-V visible (Jenway 6305UV/Vis spectrophotometer) at maximum wavelength, 504 nm for crystal violet and 466 nm for methyl orange. Experiments were repeated for different initial dye concentration (5, 10, 20, 30 and 40 mg g⁻¹) and temperature (23, 30, 40 and 50°C) values.

The removal efficiency (E) of dye on skin almonds, the sorption capacity (q) and distribution ratio (K_d) were calculated by the following equations:

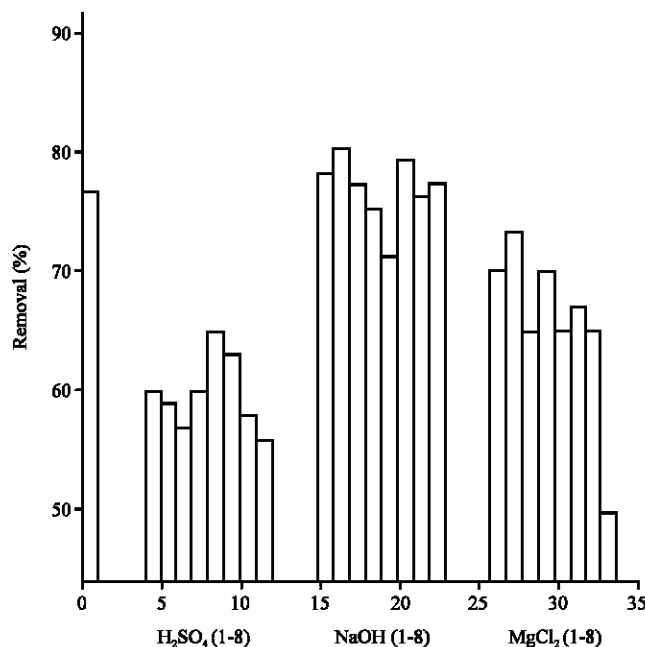


Fig. 2: Effect of chemical treatment on the adsorption of crystal violet

$$E(\%) = \frac{C_i - C_f}{C_i} \times 100 \quad (1)$$

$$q = \frac{V(C_i - C_f)}{m} \quad (2)$$

$$K_d = \frac{\text{Amount of dye in adsorbent}}{\text{Amount of dye in solution}} \times \frac{V}{m} \text{ (L g}^{-1}\text{)} \quad (3)$$

where, C_i and C_f are the initial and final concentrations of dye (mg L^{-1}) in aqueous solution, respectively, V is the volume of the solution (L) and m represents the weight of the adsorbent (g).

RESULTS AND DISCUSSION

Effect of Initial Dye Concentration

The effect of initial crystal violet and methyl orange concentration on adsorption by skin almonds was investigated in the range of 5-40 mg L^{-1} of the initial dye concentration. From Fig. 3a-c, it was observed that the uptake capacity of treated skin almonds was higher than raw one. The amount of methyl orange adsorbed increases from 3.2 to 15 mg g^{-1} and 4.6 to 31.25 mg g^{-1} as the initial adsorbate concentration increases from 5 to 40 mg L^{-1} for natural and treated skin almonds, respectively.

The experimental results showed that the removal of the dye was highly concentration dependent. The increase in uptake capacity of the sorbent with increasing dye concentration may be due to the increase of sorbate quantity. At lower initial dye concentrations, sufficient

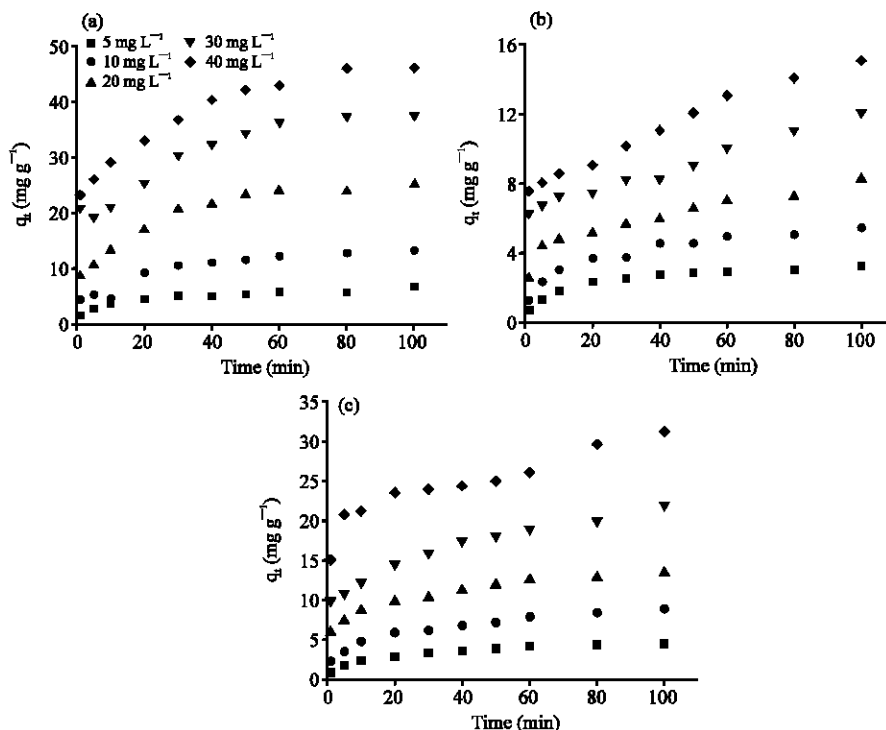


Fig. 3: Effect of time and initial dye concentration on adsorption capacity (a) CV-NSA (b) MO-NSA and (c) MO-TSA

adsorption sites are available for the sorption of dye ions. Conversely, the numbers of dye ions at higher initial concentrations are relatively more as compared to the available adsorption sites. As highlighted earlier, the difference in the removal capacity is a result of the difference in their chemical affinities and ion exchange capacity with respect to the chemical functional group on the surface of the adsorbent. In this case, the availability of free adsorption sites dominates (Ajay *et al.*, 2005).

Effect of Temperature

Temperature is a highly significant parameter in adsorption process, this dependence of these two dyes was studied with a constant initial concentration of 20 mg L⁻¹. The adsorption studies were carried out at four different temperatures 23, 30, 40 and 50°C for these three systems and the results are shown in Fig. 4a-c. On increasing the temperature of the reaction from 23 to 50°C, the amount of crystal violet on natural skin almonds, methyl orange on natural skin almonds and methyl orange on treated skin almonds decreased from 46.08 to 21; 14.7 to 10.4 and 23 to 15 mg g⁻¹, respectively similar result was also observed for methyl orange removal from wastewater using De-oiled Soya and Bottom Ash (Mittal *et al.*, 2007).

The retention capacity of the skin almonds is enhanced with decreasing temperature it indicates that the adsorption reaction is exothermic in nature.

The effect of temperature on the adsorption of crystal violet is more than the effect of temperature on the adsorption of methyl orange. These results indicate that these two dyes escape to the liquid phase from the solid phase with the rise in temperature.

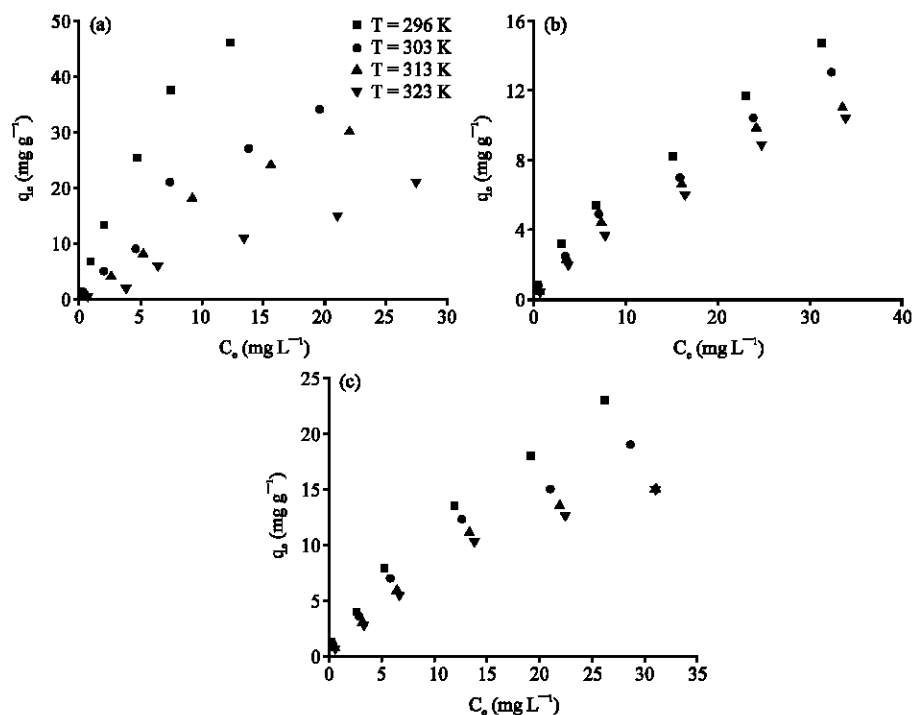


Fig. 4: Dye adsorption at various temperatures (a) CV-NSA (b) MO-NSA and (c) MO-TSA

Equilibrium Modelling

The isotherms data were analyzed using two of the most commonly used equilibrium models (Lin *et al.*, 2008; Tan *et al.*, 2008).

The Langmuir equation is given in the following equation:

$$q_e = q_{max} \frac{bC_e}{1 + bC_e} \quad (4)$$

where, q_e the amount adsorbed at equilibrium (mg g^{-1}), q_{max} the maximum amount of sorbate per unit weight of adsorbent (mg g^{-1}), C_e the concentration of adsorbate at equilibrium (mg L^{-1}) and b (L mg^{-1}) is the constant related to the affinity of the binding sites. q_{max} and b can be determined from the linear plot of C_e/q_e versus C_e .

The Freundlich equation is an empirical equation employed to describe heterogeneous systems, in which it is characterized by the heterogeneity factor $1/n$. Hence the empirical equation can be written:

$$q_e = K_f \cdot C_e^{1/n} \quad (5)$$

where, K_f is the Freundlich constants and $1/n$ is a measure of the adsorption intensity. Equation 5 can be linearized in logarithmic form and the Freundlich constants can then be determined.

The essential characteristics of the Langmuir isotherm can be expressed in terms of a dimensionless constant separation factor R_L (Batzias and Sidiras, 2004) as:

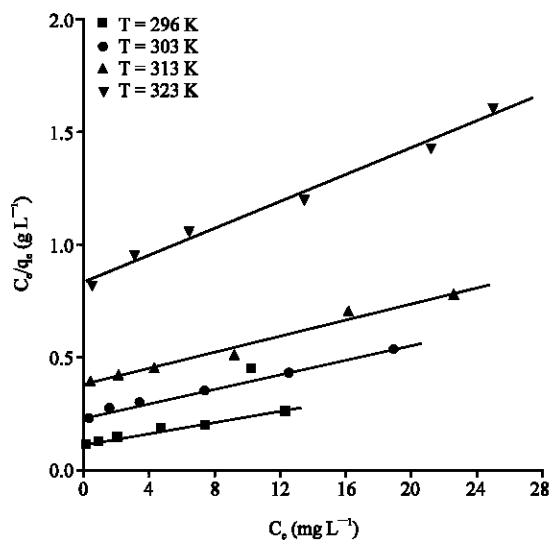


Fig. 5: Langmuir adsorption isotherm for CV-NSA at various temperatures

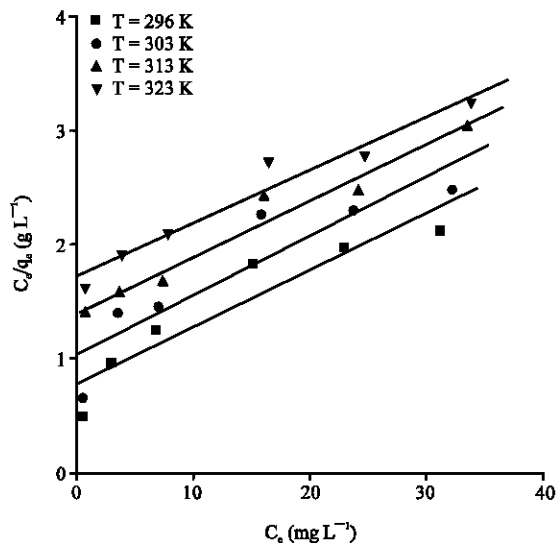


Fig. 6: Langmuir adsorption isotherm for MO-NSA at various temperatures

$$R_L = \frac{1}{1 + bC_e} \tag{6}$$

Figure 5-10 show the fitted equilibrium data in Freundlich and Langmuir expressions. The isotherm parameters and the correlation coefficients (R^2) are shown in Table 2.

A comparison of the experimental isotherms with the adsorption isotherm models showed that the Langmuir equation represented the poorest fit of experimental data as compared to the isotherm Freundlich equation ($R^2 > 0.99$) for systems MO-NSA and MO-TSA.

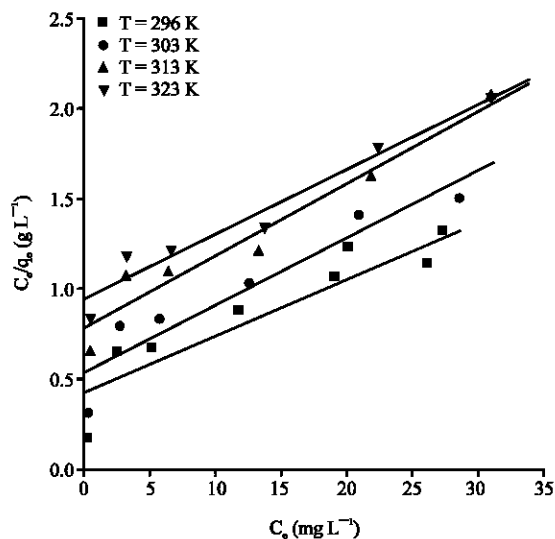


Fig. 7: Langmuir adsorption isotherm for MO-TSA at various temperatures

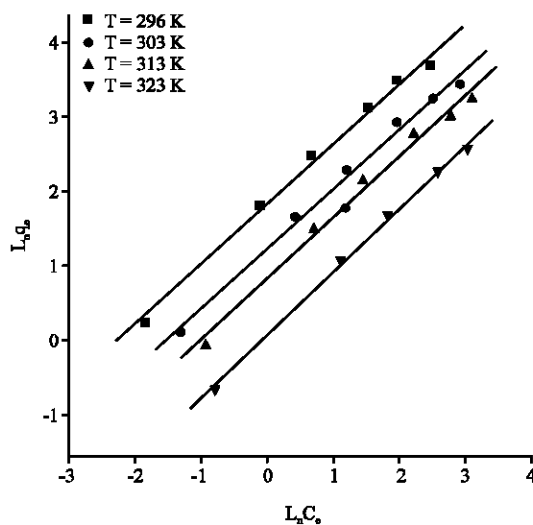


Fig. 8: Freundlich adsorption isotherm for CV-NSA at various temperatures

It is clear from Table 2 that the values of n were greater than 1, indicating favourable adsorption condition. Both K_f and n reached their corresponding maximum values, at 23°C. This implies that binding capacity reaches the highest value and the affinity between the sorbent and dye ions was also higher than other temperature values investigated. The constant b represents affinity between the sorbent and sorbate, b increases with decreasing temperature from 23 to 50°C.

It can be observed that the corresponding q_{max} values of the system MO/untreated skin almonds for 23-50°C temperature range were not affected with changes of temperature solution.

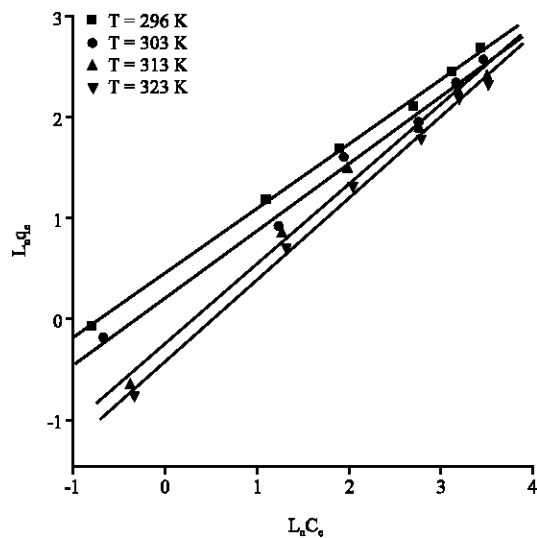


Fig. 9: Freundlich adsorption isotherm for MO-NSA at various temperatures

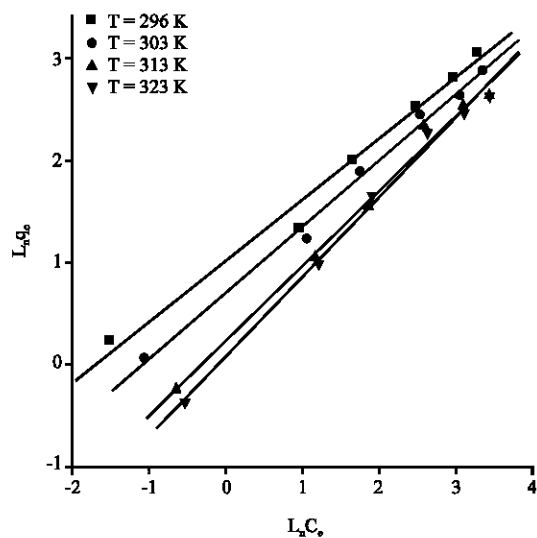


Fig. 10: Freundlich adsorption isotherm for MO-TSA at various temperatures

The value of R_L indicates whether the isotherm is irreversible ($R_L = 0$), favourable ($0 < R_L < 1$), unfavourable ($R_L > 0$). The results are shown in Fig. 11 and 12. It was found that the value of R_L is between 0.205 and 0.728 for all systems studied and confirmed that the treated and untreated skin almonds is favourable for adsorption of methyl orange and crystal violet under conditions used in this study.

Adsorption Kinetics

Pseudo Second Order Model

Based on equilibrium adsorption, the pseudo second-order kinetic equation (Kavitha and Namasivayam, 2007a, b) is expressed as:

Table 2: Freundlich and Langmuir isotherm model constants and correlation coefficients

T (°C)	K _F	n	R ²	q ₀ (mg g ⁻¹)	b (L mg ⁻¹)	R ²
Crystal violet						
Natural skin almonds						
23	6.87	1.218	0.997	85.47	0.097	0.989
30	3.74	1.230	0.996	63.69	0.065	0.995
40	3.14	1.360	0.994	55.24	0.048	0.990
50	1.53	1.350	0.998	33.78	0.035	0.993
Methyl orange						
Natural skin almonds						
23	1.513	1.538	0.999	20.24	0.063	0.880
30	1.196	1.483	0.996	19.23	0.050	0.832
40	0.749	1.248	0.994	20.21	0.035	0.961
50	0.628	1.219	0.998	21.10	0.027	0.951
Treated skin almonds						
23	2.916	1.647	0.984	31.94	0.074	0.815
30	2.122	1.531	0.993	26.73	0.070	0.894
40	1.306	1.335	0.990	24.57	0.053	0.945
50	1.128	1.270	0.993	27.10	0.040	0.956

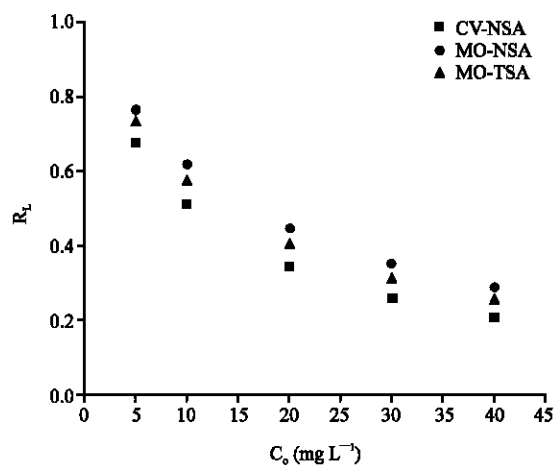


Fig. 11: Separation factor at 23°C at various dye concentrations

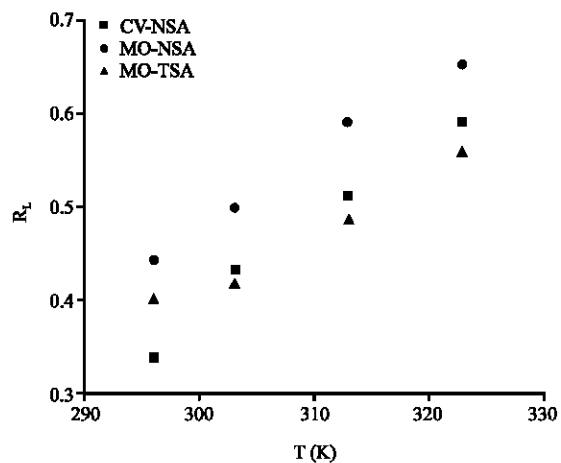


Fig. 12: Separation factor at various temperatures

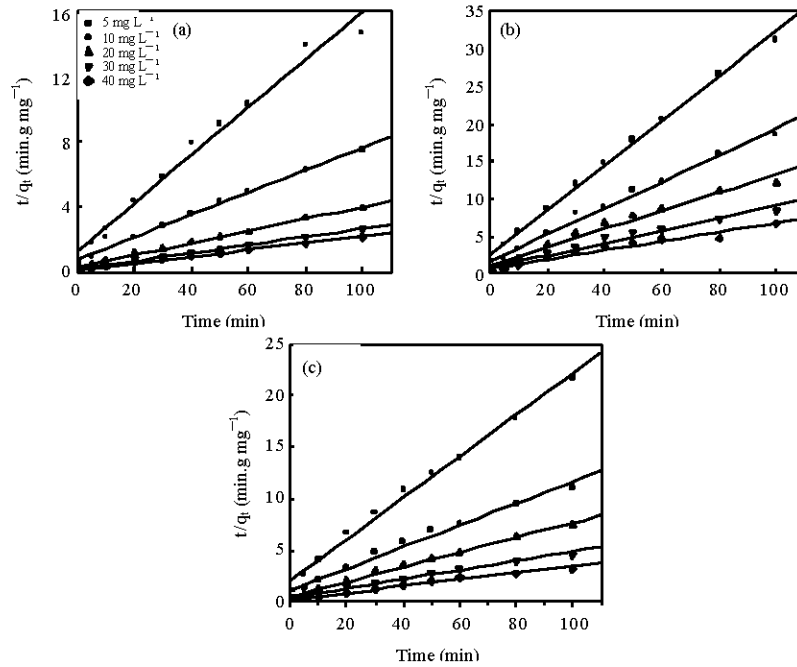


Fig. 13: Pseudo-second-order kinetics for the sorption of dye at 23°C (a) CV-NSA, (b) MO-NSA and (c) MO-TSA

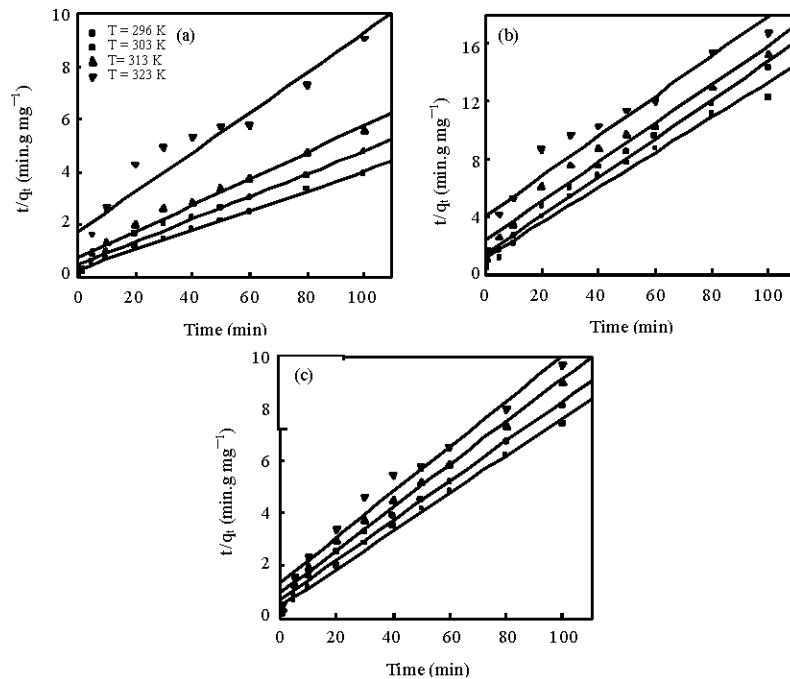


Fig. 14: Pseudo-second-order kinetics for the sorption of dye at various temperatures (a) CV-NSA, (b) MO-NSA and (c) MO-TSA

$$\frac{t}{q_t} = \frac{1}{k_2 q_e^2} + \frac{t}{q_e} \tag{7}$$

where, K_2 is the rate constant of pseudo-second order adsorption (g mg min^{-1}).

The initial adsorption rate, h , (mg gmin^{-1}) is expressed as:

$$h = K_2 q_e^2 \tag{8}$$

The application of the linear form of pseudo-second-order kinetic model on our experimental results is shown in Fig. 13a-c and 14a-c. Both constants K_2 and h were calculated from the intercept and slope of the line obtained by plotting t/q_t versus t . It can be shown from Table 3 that the kinetics of dye adsorption onto skin almonds (treated and untreated) follow this model with correlation coefficients higher than 0.99. Further, the rate constant, K_2 , decreased with increase in initial dye concentration. Similar phenomena had been observed in the adsorption of methylene blue by hazelnut shells and wood sawdust (Ferreiro, 2007), acid blue 193 onto BTMA-bentonite (Ozcan *et al.*, 2005) and adsorption of basic black dye using calcium alginate beads (Aravindhan and Nishtar, 2007).

Table 3: Comparison of the pseudo-second-order and intraparticle diffusion models of crystal violet on natural skin almonds

C_0 (mg L^{-1})	T ($^{\circ}\text{C}$)	$q_{e,exp}$ (mg g^{-1})	Pseudo-second-order kinetic				Intraparticle diffusion			
			$q_{e,cal}$ (mg g^{-1})	k_2 (g mg min^{-1})	h (g mg min^{-1})	R^2	Δq_t (%)	k_{id} ($\text{g min}^{-0.5}$)	R^2	Δq_t (%)
Crystal violet										
Natural skin almonds										
5	23	6.80	6.77	0.0169	0.774	0.981	6.79	0.51	0.931	7.76
10	23	13.28	14.49	0.0063	1.322	0.981	6.43	1.12	0.910	17.80
20	23	25.39	26.88	0.0046	3.323	0.993	6.68	2.01	0.938	8.04
30	23	37.51	39.68	0.0038	5.983	0.992	9.24	2.38	0.928	7.34
40	23	46.08	48.08	0.0034	7.859	0.994	7.86	2.79	0.975	3.37
20	23	25.39	26.88	0.0046	3.323	0.993	6.68	2.01	0.938	8.04
20	30	21.00	23.25	0.0037	2.000	0.983	10.26	1.86	0.963	10.35
20	40	18.00	19.96	0.0034	1.354	0.978	8.47	1.70	0.975	5.79
20	50	11.00	13.26	0.0032	0.562	0.913	16.49	1.01	0.951	15.40
Methyl orange										
Natural skin almonds										
5	23	3.2	3.36	0.0353	0.398	0.996	2.97	0.270	0.966	8.63
10	23	5.4	5.65	0.0189	0.603	0.988	8.36	0.438	0.933	6.37
20	23	8.2	8.22	0.0133	0.898	0.979	14.24	0.546	0.958	5.37
30	23	12.0	12.00	0.0089	1.288	0.963	17.50	0.624	0.944	8.10
40	23	15.0	6.47	0.0053	1.437	0.946	18.25	0.879	0.909	4.12
20	23	8.2	8.22	0.0133	0.898	0.979	14.24	0.546	0.958	5.37
20	30	7.0	7.50	0.0123	0.691	0.985	10.86	0.592	0.967	9.93
20	40	6.6	7.40	0.0077	0.421	0.964	12.29	0.632	0.985	4.87
20	50	6.0	7.19	0.0048	0.248	0.928	12.90	0.618	0.988	6.52
Treated skin almonds										
5	23	4.6	4.95	0.0208	0.509	0.991	6.82	0.396	0.953	5.78
10	23	9.0	9.44	0.0105	0.935	0.985	7.91	0.717	0.973	5.34
20	23	13.5	13.88	0.0117	2.254	0.993	7.99	0.827	0.973	3.20
30	23	22.0	22.32	0.0055	2.740	0.985	9.74	1.364	0.992	2.43
40	23	31.2	31.05	0.0052	5.013	0.981	13.85	1.489	0.926	4.64
20	23	13.5	13.88	0.0117	2.254	0.993	7.99	0.827	0.973	3.20
20	30	12.3	13.17	0.0082	1.422	0.990	7.58	0.992	0.966	5.57
20	40	11.1	12.16	0.0070	1.214	0.987	7.28	0.983	0.975	5.92
20	50	10.3	11.54	0.0055	0.732	0.972	9.96	0.975	0.986	5.93

The variations of t/q_t versus t at various temperatures of dye solution under the initial concentration of 20 mg L^{-1} still confirmed to fit the pseudo-second-order model. The values of model parameters (K_2 , h and q_e) for different temperatures have been calculated from Eq. 7 and 8 and the results are shown in Table 3, revealing that the fitted adsorption capacity at equilibrium, q_e , decreased with increasing temperature. The values of the initial sorption rate, h , increases from 0.777 to 7.856 as the solution concentration increases from 5 to 40 mg L^{-1} and decreases with increasing temperature for these three systems (CV-NSA, MO-NSA and MO-TSA).

These results imply that physic-sorption mechanism may play an important role for the adsorption of each dye on the raw and treated skin almonds. Based on the values of R^2 shown in Table 3, it is clear that the pseudo-second-order equation is better in describing the adsorption kinetics.

Intra-Particle Diffusion Model

The pseudo-second-order kinetic model could not identify the diffusion mechanism and the kinetic results were then analyzed by using the intraparticle diffusion model. Although, the kinetic studies help in identifying the adsorption process, the determination of the adsorption mechanism is important for design purposes. There is a possibility that the transport of the crystal violet or methyl orange from the solution into the pores of adsorbent is rate controlling. Hence, the data was further processed for testing the role of diffusion in the adsorption process.

In the model developed by Indra *et al.* (2006), the initial rate of intra-particle diffusion is calculated by linearization of the Eq. 9:

$$q_t = K_i t^{1/2} + C \quad (9)$$

where, C (mg g^{-1}) is the intercept and K_i is intra-particle diffusion rate constant ($\text{mg g min}^{-1/2}$). According to this model, the plot of uptake, q_t versus the square root of time ($t^{1/2}$) should be linear if intraparticle diffusion is involved in the adsorption process and if these lines pass through the origin then intraparticle diffusion is the rate controlling step.

The deviation of straight lines from the origin (Fig. 15a-c, 16a-c) indicates that the pore diffusion is not the sole rate controlling step. The values of rate constants (K_i) are shown in Table 3. The intraparticle diffusion, K_i , values were obtained from the slope of the straight line portions of plot of q_t versus $t^{1/2}$ for various dye concentrations and solutions temperature (Fig. 15, 16). It was observed that intraparticle rate constant values (K_i) increased with initial dye concentration. The increase in K_i values with increasing initial dye concentration can be explained by the growing effect of driving force resulted in reducing the diffusion of dye species in the boundary layer and enhancing the diffusion in the solid. Also, as shown in Table 3, increasing the temperature decreased the pore diffusion in sorbent particles.

Test of Kinetic Models

In order to quantitatively compare the applicability of each model in fitting to data a normalized standard deviation, Δ_q was calculated:

$$\Delta q(\%) = 100 \sqrt{\frac{\sum [(q_{t, \text{exp}} - q_{t, \text{cal}}) / q_{t, \text{exp}}]^2}{N-1}} \quad (10)$$

where, the $q_{t, \text{exp}}$ and $q_{t, \text{cal}}$ are the experimental and calculated values and N is the number of data points.

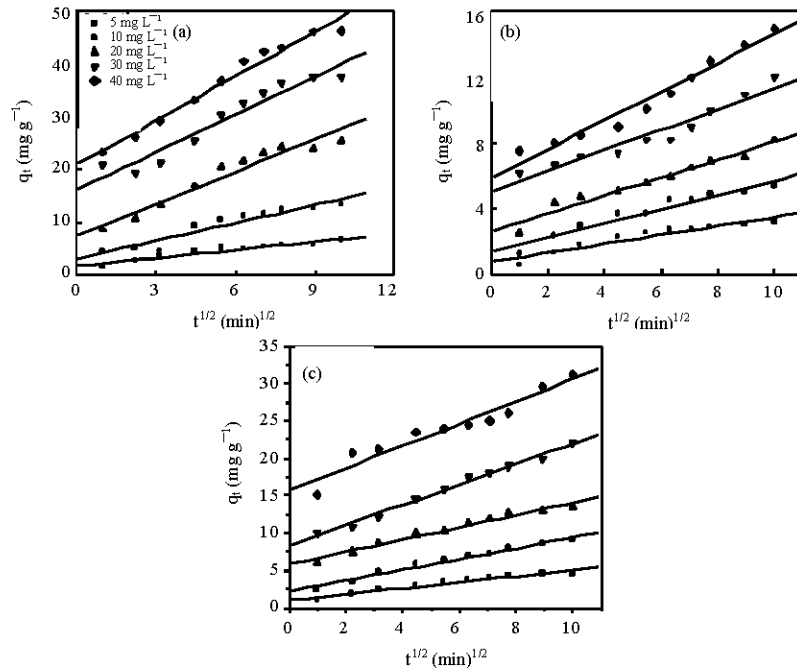


Fig. 15: Plots of intraparticle diffusion modelling for the sorption of dye at 23°C (a) CV-NSA, (b) MO-NSA and (c) MO-TSA

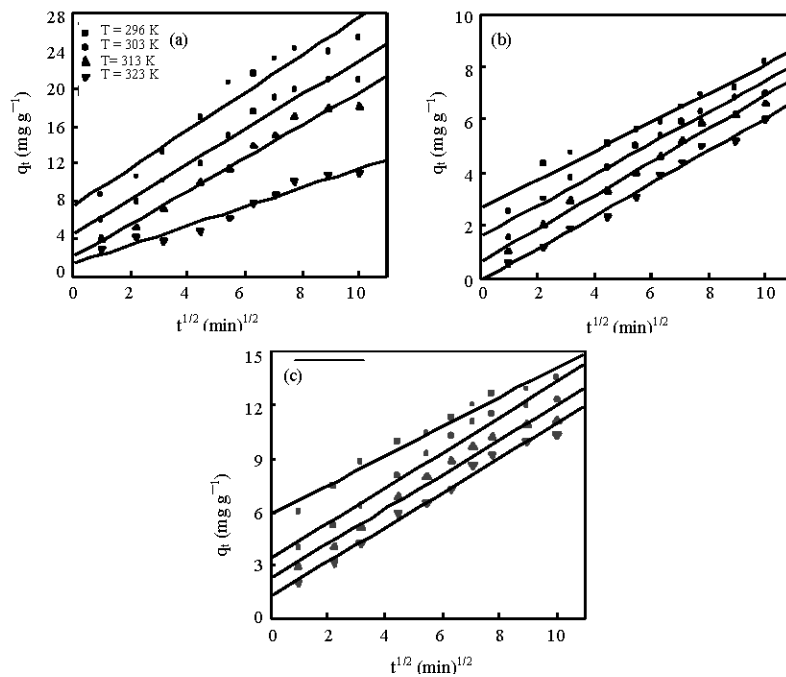


Fig. 16: Plots of intraparticle diffusion modelling for the sorption of dye at various temperatures (a) CV-NSA, (b) MO-NSA and (c) MO-TSA

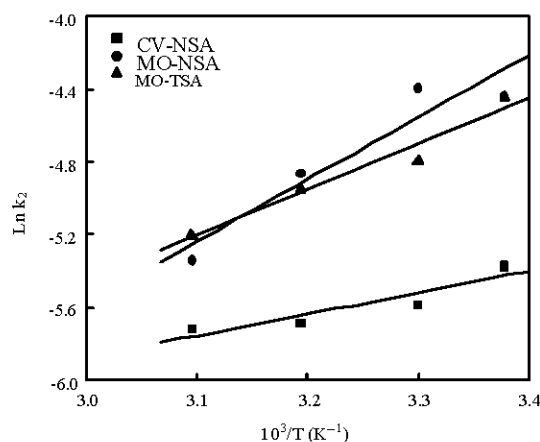


Fig. 17: Arrhenius plots for adsorption of crystal violet and methyl orange at various temperatures

Theoretical calculated values of the remaining sorption capacities of each dye were found to have a close agreement with the experimentally-measured values for the pseudo second as compared to the intraparticle model (Table 3). Based on the values of R^2 and Δq given in Table 3, it is clear that the pseudo-second-order equation is better in describing the adsorption kinetics.

Thermodynamic Parameters

The thermodynamic parameters of the adsorption process were determined from the experimental data obtained using the following equations (Kavitha and Namasivayam, 2007a, b):

$$K_2 = K_0 e^{\left[\frac{-E_a}{RT}\right]} \quad (11)$$

$$\Delta G^\circ = -RT \ln K_d \quad (12)$$

$$\ln K_d = -\frac{\Delta H^\circ}{RT} + \frac{\Delta S^\circ}{R} \quad (13)$$

where, K_d is the distribution coefficient for the adsorption, ΔS° , ΔH° and ΔG° are the change of entropy, enthalpy and the Gibbs energy, T is the absolute temperature, R is the gas constant.

The second-order rate constant is expressed as a function of temperature by the Arrhenius equation (Eq. 11). K_0 is the temperature independent factor (g mg min^{-1}); E_a is the activation energy of sorption (kJ mol^{-1}). The activation energy values were calculated to be -9.688 , -28.189 and $-20.951 \text{ kJ mol}^{-1}$ for CV-NSA, MO-NSA and MO-TSA, respectively (Fig. 17).

These results (Table 4) show that these dyes adsorption process by skin almonds natural or treated were exothermic. This low value of activation energy suggested that the adsorption process was governed by the physisorption (Hameed *et al.*, 2007). The values of

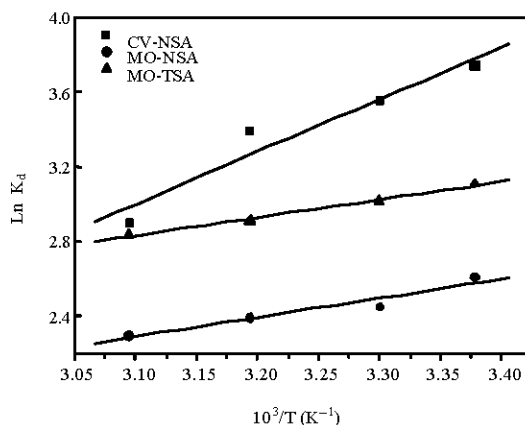


Fig. 18: Van' t Hoff plots for the adsorption of crystal violet and methyl orange

Table 4: Thermodynamic parameters

Systems	ΔG° (kJ mol ⁻¹)				ΔH° (kJ mol ⁻¹)	ΔS° (J mol ⁻¹ K)
	23	30	40	50		
CV-NSA	37.19	37.52	38.00	38.46	23.25	47.11
MO-NSA	10.71	10.76	10.83	10.90	8.52	7.37
MO-TSA	8.25	8.26	8.27	8.28	7.94	1.05

ΔH° and ΔS° were determined from the slope and intercept of the plot of $\text{Ln}K_d$ vs. $1/T$ (Fig. 18). ΔH° and ΔS° values are all negative for adsorption of these three systems. The negative value of ΔG° indicated the feasibility of the process and the spontaneous nature of the adsorption; while the negative value of ΔS° suggested that this adsorption would lead to decreasing randomness.

CONCLUSION

The skin almonds, an agriculture waste were successfully employed in natural form for removal of basic dye and with H_2SO_4 treatment for removal of acid dye. The removal of crystal and methyl orange were systematically investigated under various conditions. From the results, it could be concluded that the adsorption was dependent on initial concentration and temperature solution. The maximum adsorption capacities of crystal violet onto skin almond and methyl orange onto natural and treated skin almond were 85.47, 21.10 and 31.94 mg g⁻¹, respectively and for the temperature of 23°C. Adsorption equilibrium for these three systems on untreated and treated skin almonds was best represented by the Freundlich isotherm. Two kinetic models, pseudo-second-order and intraparticle diffusion were tested to investigate the adsorption mechanism. The experimental data fitted very well the pseudo second order kinetic model and also followed by intraparticle diffusion model for all initial concentrations and temperatures. The thermodynamics data shows the process is exothermic and spontaneous nature.

REFERENCES

Ajay, K.M., G.K. Mishra, P.K. Rai, R. Chitra and P.N. Nagar, 2005. Removal of heavy metal ions from aqueous solutions using carbon aerogel as an adsorbent. *J. Hazard. Mater.*, B122: 161-170.

- Aksu, Z., 2005. Application of biosorption for the removal of organic pollutants: A review. *Process Biochem.*, 40: 997-1026.
- Aksu, Z. and S. Tezer, 2005. Biosorption of reactive dyes on the green alga *Chlorella vulgaris*. *Process Biochem.*, 40: 1347-1361.
- Aravindhan, R. and N.F. Nishtar, 2007. Equilibrium and thermodynamic studies on the removal of basic dye using calcium alginate beads. *Colloids Surfaces A: Physicochem. Eng. Aspect*, 299: 232-238.
- Batzias, F. and D.K. Sidiras, 2004. Dye adsorption by calcium-chloride treated beech sawdust in batch and fixed bed systems. *J. Hazard. Mater.*, B114: 167-174.
- Ferferro, F., 2007. Dye removal by low cost adsorbents: Hazelnut shells in comparison with wood sawdust. *J. Hazard. Mater.*, 142: 144-152.
- Forgacs, E., T. Cserhati and G. Oros, 2004. Removal of synthetic dyes from wastewater: A review. *Environ. Int.*, 30: 953-971.
- Fu, Y. and T. Viraraghavan, 2001. Fungal decolorization of dyewastewater: A review. *Biores. Technol.*, 79: 251-262.
- Grini, G., H.N. Peindy, F. Gimbert and C.F. Robert, 2007. Removal of C.I. Basic Green 4 (Malachite Green) from aqueous solutions by adsorption using cyclodextrin-based adsorbent: Kinetic and equilibrium studies. *Separation Purificat. Technol.*, 53: 97-110.
- Gurses, A., C. Dogar, M. Yalcin, M. Acikyildiz, R. Bayrak and S. Karaca, 2006. The adsorption kinetics of the cationic dye, methylene blue, onto clay. *J. Hazard. Mater.*, B131: 217-228.
- Hamdaoui, O., 2006. Batch study of liquid-phase adsorption of methylene blue using cedar sawdust and crushed brick. *J. Hazard. Mater.*, B135: 264-273.
- Hameed, B.H., A.A. Ahmad and N. Aziz, 2007. Isotherms, kinetics and thermodynamics of acid dye adsorption on activated palm ash. *Chem. Eng. J.*, 133: 195-203.
- Indra, D., M. Vimal, C. Srivastava and N.K. Agarwal, 2006. Removal of orange-G and methyl violet dyes by adsorption onto bagasse fly ash-kinetic study and equilibrium isotherm analysis. *Dyes Pigments*, 69: 210-223.
- Kavitha, D. and C. Namasivayam, 2007a. Recycling coir pith, an agricultural solid waste, for the removal of procion orange from wastewater. *Dyes Pigments*, 74: 237-248.
- Kavitha, D. and C. Namasivayam, 2007b. Experimental and kinetic studies on methylene blue adsorption by coir pith carbon. *Bioresour. Technol.*, 98: 14-21.
- Lin, J.X., Zhan, M.H. Fang, M.H. Qian, X.Q. Yang and H. Xang, 2008. Adsorption of basic dye from aqueous solution onto fly ash. *J. Environ. Manage.*, 87: 193-200.
- Mittal, A., A. Malviya, D. Mittal and L. Kurup, 2007. Studies on the adsorption kinetics and isotherms for the removal and recovery of methyl orange from wastewater using waste materials. *J. Hazard. Mater.*, 148: 229-240.
- Namasivayam, C., M.D. Kumar, K. Selvi, R.A. Begum, T. Vanathi and R.T. Yamuna, 2001. Waste coir pith: A potential biomass for the treatment of dyeing wastewater. *Biomass Bioenergy*, 21: 477-483.
- Ozcan, A.S., B. Erdem and A. Ozcan, 2005. Adsorption of acid blue 193 from aqueous solution onto BTMA-bentonite. *Colloids Surfaces A: Physicochem. Eng. Aspect*, 266: 73-81.
- Tan, I.A.W., A.L. Ahmad and B.H. Hameed, 2008. Enhancement of basic dye adsorption uptake from aqueous solutions using chemically modified oil palm shell activated carbon. *Colloids Surfaces A: Physicochem. Eng. Aspects*, 318: 88-96.
- Wua, F.C., R.L. Tseng and R.S. Juang, 2005. Preparation of highly microporous carbons from fir wood by KOH activation for adsorption of dyes and phenols from water. *Separation Purification Technol.*, 47: 10-19.
- Yeddou, N. and A. Bensmaili, 2007. Equilibrium and kinetic modelling of iron adsorption by eggshells in a batch system: Effect of temperature. *Desalination*, 206: 127-134.